3% in patients with chronic hepatitis and 30% in those with cirrhosis. For the chronic hepatitis patients, the log-rank test showed the significant risk factors related to HCC development to be age ≥50 years, platelet count $<14.0 \times 10^4/mm^3$, and hepatitis B e antigen negativity, but median HBV-DNA levels of <4.0 log copies/ml (maintained viral response, MVR) did not significantly suppress the development of HCC. In cirrhosis patients, however, the attainment of MVR during LAM treatment was revealed to reduce the risk of HCC development.

Conclusions These results suggest that the incidence of HCC in HBV patients with cirrhosis can be reduced in those with an MVR induced by consecutive LAM treatment.

Keywords Lamivudine · Chronic hepatitis B · Cirrhosis · Hepatocellular carcinoma · HBV-DNA level

Abbreviations

HBV	Hepatitis B virus
HCC	Hepatocellular carcinoma
LAM	Lamivudine
ADV	Adefovir
ETV	Entecavir
Hbs Ag	Hepatitis B surface antigen
PCR	Polymerase chain reaction
TMA	Transcription-mediated amplification
IVR	Initial viral response
MVR	Maintained viral response
HBe Ag	Hepatitis B e antigen
CT	Computed tomography
MRI	Magnetic resonance imaging
ALT	Alanine aminotransferase

Introduction

More than 350 million people worldwide suffer from chronic infection with hepatitis B virus (HBV) [1–3]. Chronic HBV infection eventually leads to the development of cirrhosis and hepatocellular carcinoma (HCC), and raises the risk of hepatic disease-related death [4–6]. In Japan, up to 15% of HCC patients are diagnosed with HBV-related liver disease [7].

HCC is one of the most common malignancies in Japan and its incidence has been increasing over the past 30 years. Recently, various treatments such as transcatheter arterial embolization/chemoembolization, radio-frequency ablation, and hepatic resection have been reported to yield significant improvements in overall patient survival [8–11]. However, HCC relapse has thus far been observed in a majority of treated patients due to its highly malignant potential. In this regard, successful treatment of chronic HBV infection should prevent the patient's liver from progressing to cirrhosis and reduce the risk of HCC development. In recent years, the treatment of chronic hepatitis has changed greatly with the development of various antiviral therapies with nucleoside/nucleotide analogues such lamivudine (LAM), adefovir (ADV), and entecavir (ETV) [12–15]. LAM has long been used against chronic hepatitis, and many reports have demonstrated that LAM is effective in stabilizing inflammatory activity, suppressing HBV-DNA replication, and improving liver histological findings in chronic hepatitis patients [16, 17] and in HBV-related cirrhosis patients [18]. Furthermore, LAM has been reported to reduce the incidence of HCC in patients with chronic hepatitis B [19]. However, it is still controversial whether or not treatment using nucleotide analogues can reduce the risk of HCC development in HBV-infected patients [20, 21], and the relationship between the effect of HBV suppression and HCC development during LAM treatment has not yet been discussed in detail. Also, the risk factors for HCC development in HBV-infected patients who have been treated with LAM have not been sufficiently evaluated. In this study, we aimed to clarify whether the decrease of HBV-DNA amount induced by LAM therapy could reduce the incidence of HCC in HBV-infected patients.

Patients and methods

Patient selection and study design

This study was conducted at Osaka University Hospital and other institutions participating in the Osaka Liver Forum in Japan. The subjects were 293 consecutive patients with HBV infection who underwent continuous LAM therapy for more than 24 weeks from September 2000 to September 2006. All patients tested positive for hepatitis B surface antigen (HBs Ag) or had detectable levels of HBV DNA in their sera according to findings from a polymerase chain reaction (PCR)-based method or a transcription-mediated amplification (TMA) method. Exclusion criteria were patients with anti-hepatitis C antibody, anti-human immunodeficiency virus antibody, and other liver diseases (alcoholic liver disease, drug-induced liver disease, and autoimmune hepatitis). Also excluded were patients with a history of HCC and those who developed HCC within the first 24 weeks of the follow-up period after the initiation of LAM therapy (because of the possibility that microscopic HCC had been present before the initiation of treatment).

All patients were treated with 100 mg of LAM daily. Of the 293 patients, 129 underwent ADV (10 mg/day) therapy in addition to receiving ongoing LAM treatment. For 43 patients who started ETV administration in lieu of LAM, the observation period was terminated when they started

ETV. LAM resistance was confirmed by virological breakthrough and was defined as an increase in serum HBV-DNA by >1 $\log_{10}$ greater than the nadir [22]. If virological breakthrough developed and alanine aminotransferase (ALT) was elevated over the upper normal limit, the patients received add-on ADV at 10 mg/day.

In this study, all patients were examined for serum HBV-DNA level just before therapy initiation and every 6 months during treatment. The initial viral response (IVR) was defined as HBV-DNA <4.0 log copies/ml in the first 24 weeks of the follow-up period after the initiation of LAM therapy, and the maintained viral response (MVR) was defined as median HBV-DNA levels of less than 4.0 log copies/ml measured every 6 months during therapy.

This study protocol followed the ethical guidelines of the Declaration of Helsinki amended in 2008, and informed consent was obtained from each patient.

HBV testing

HBs Ag, hepatitis B e antigen (HBe Ag) and anti-hepatitis B e antibody (anti-HBe) levels were examined by chemiluminescence immunoassay or enzyme immunoassay. HBV DNA was measured by a PCR-based method (Amplicor HBV monitor; Roche Diagnostics, Tokyo, Japan) or a TMA method (TMA-HPA; Fujirebio, Tokyo, Japan), which have lower detection limits of 2.6 and 3.7 log copies/ml, respectively. The LAM-resistant YMDD mutant virus was examined by a PCR-ELMA method. Serum samples were stored frozen at −80°C.

Diagnosis of HCC and cirrhosis

Ultrasonography was carried out before LAM therapy and every 3–6 months during the follow-up period. New space-occupying lesions detected or suspected at the time of ultrasonography were further examined by computed tomography (CT), magnetic resonance imaging (MRI), or hepatic angiography. HCC was diagnosed by the presence of typical hypervascular characteristics on angiography, in addition to the findings from CT or MRI. If no typical image of HCC was observed, fine-needle aspiration biopsy was carried out with the patient's consent or the patient was carefully followed until a diagnosis was possible with definite observation by CT, MRI, or hepatic angiography. Cirrhosis was diagnosed by liver biopsy or laparoscopy, and for patients without this information, by clinical data, imaging modalities, and portal hypertension.

Statistical analysis

Quantitative variables were expressed as means ± SD. Quantitative variables at the baseline were compared among two groups, the chronic hepatitis and cirrhosis groups, using the Mann–Whitney *U*-test. Categorical data, such as gender and status of HBe Ag, were compared using Fisher's exact test. The cumulative incidence of HCC was evaluated with a Kaplan–Meiercurve and the differences between groups were analyzed by the log-rank test. For multivariate analysis to investigate factors affecting the cumulative incidence of HCC, Cox's regression analysis was carried out. A value of $p < 0.05$ (two-tailed) was considered to be statistically significant. All calculations were performed with SPSS version 15.0J (SPSS, Chicago, IL, USA).

Results

Baseline characteristics of patients

The baseline clinical features of the enrolled patients before LAM administration are shown in Table 1. The mean age of the patients was 48.0 ± 10.7 years, 214 (73%) of the entire group were male, and 163 (56%) tested positive for HBe Ag. Of the 293 patients, 205 (70%) were diagnosed as having chronic hepatitis and 88 (30%) as having cirrhosis. The median HBV-DNA level was 7.0 (range 3.0 to 8.5<) log copies/ml. At baseline, the aspartate aminotransferase (AST) level was 131 ± 151 IU/l, the ALT level was 203 ± 252 IU/l, the total bilirubin level was 1.2 ± 1.6 mg/dl, the albumin (Alb) level was 3.8 ± 0.5 g/dl, and the platelet count was 13.7 ± 5.4 × 10^4/mm^3. The mean follow-up period for all patients was 67.6 ± 27.4 months, with a range of 12–110 months from the start of LAM treatment. There were significant differences between patients with chronic hepatitis and those with liver cirrhosis in age, AST, ALT, total bilirubin, Alb, and platelet counts.

Cumulative incidence of development of HCC

Figure 1a shows the Kaplan–Meier curve of the cumulative HCC incidence for all HBV patients treated with LAM or LAM plus ADV. Of the 293 patients with HBV infection, 32 (10.9%) developed HCC and the cumulative carcinogenesis rate was 6% at 3 years, 12% at 5 years, and 15% at 7 years.

Figure 1b shows the Kaplan–Meier curve of the cumulative HCC incidence according to initial diagnosis (chronic hepatitis vs. cirrhosis). Eight (4%) of the 205 enrolled chronic hepatitis patients developed HCC and the cumulative carcinogenesis rate was 2% at 3 years, 3% at 5 years, and 5% at 7 years. On the other hand, 24 (27%) of the 88 enrolled cirrhosis patients developed HCC and the cumulative carcinogenesis rate was 15% at 3 years, 30% at 5 years, and 35% at 7 years.

Table 1 Patient characteristics

Factor	All	Chronic hepatitis	Cirrhosis	*p* value
Number of patients	293	205	88	
Age (years)	48.0 ± 10.7	46.3 ± 10.7	51.9 ± 9.8	<0.001**
Sex (male/female)	214/79	147/58	67/21	0.475
HBe Ag (positive	163 (56%)	121 (59%)	42 (48%)	0.068
HBV DNA (log copies/ml)[a]	7.0 (3.0 to 8.5<)	6.8±1.1	6.6 ± 1.1	0.162
AST (IU/l)	131 ± 151	143 ± 162	104 ± 120	0.045*
ALT (IU/l)	203 ± 252	235 ± 269	129 ± 189	<0.001**
Total bilirubin (mg/dl)	1.2 ± 1.6	0.9 ± 0.6	1.8 ± 2.7	<0.001**
Alb (g/dl)	3.8 ± 0.5	3.9 ± 0.4	3.5 ± 0.6	<0.001**
Platelets ($\times 10^4$/mm^3)	13.7 ± 5.4	15.6 ± 9.3	9.3 ± 3.8	<0.001**
Follow-up period (months)	67.6 ± 27.4	68.5 ± 26.5	65.5 ± 29.5	0.393

HBe Ag Hepatitis B e antigen, *HBV* hepatitis B virus, *AST* aspartate aminotransferase, *ALT* alanine aminotransferase, *Alb* albumin

[a] Values are expressed as medians

* $p < 0.05$, ** $p < 0.001$, comparing patients with chronic hepatitis and those with liver cirrhosis using the Mann–Whitney *U*-test for quantitative variables and Fisher's exact test for categorical variables

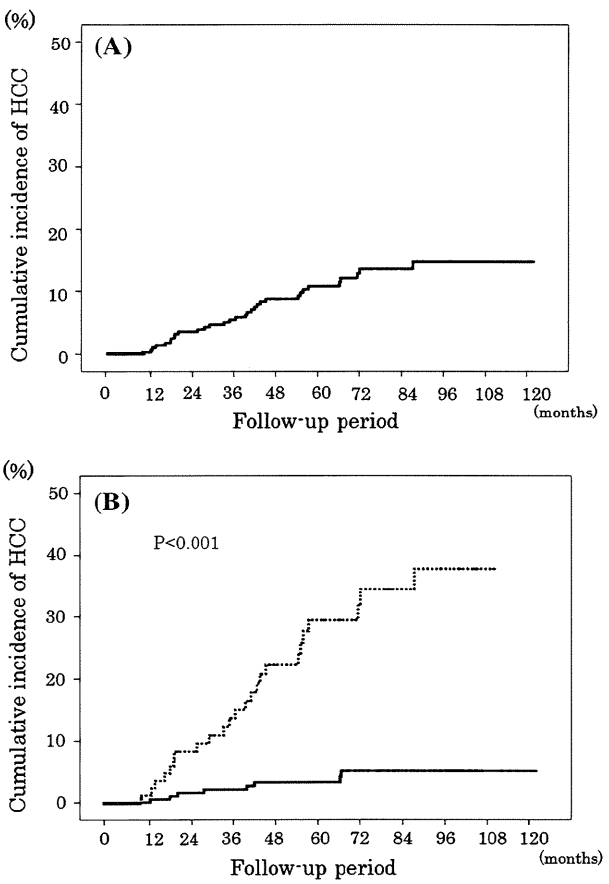

Fig. 1 Cumulative incidence of development of hepatocellular carcinoma (*HCC*) in patients with hepatitis B virus infection treated with lamivudine (LAM). **a** All cases; **b** chronic hepatitis or cirrhosis. *Solid line* Chronic hepatitis, *dotted line* cirrhosis

Risk factors for cumulative incidence of HCC development in all HBV-infected patients

Univariate analysis with the log-rank test was performed for all HBV-infected patients treated with LAM, with the results shown in Table 2. Univariate analysis with the log-rank test showed that the following were significant risk factors for the development of HCC: older age (≥50 years) ($p < 0.001$), cirrhosis ($p < 0.001$), high total bilirubin level (>1.2 g/dl) ($p = 0.004$), low Alb level (<3.8 g/dl) ($p = 0.019$), low platelet count (<14 × 10^4/mm^3) ($p < 0.001$), and non-MVR ($p = 0.035$).

Stepwise multivariate analyses of four of these variables were performed by Cox's regression analysis for all patients treated with LAM with the results shown in Table 3. The analysis indicated the following factors as independent significant risk factors related to the development of HCC: age ≥50 years [hazard ratio (HR) 3.20, 95% confidence interval [CI] 1.08–9.53, $p = 0.036$], platelet count <14.0 × 10^4/mm^3 (HR 4.76, 95% CI 0.05–0.96, $p = 0.045$), cirrhosis (HR 4.64, 95% CI 1.75–12.4, $p = 0.002$), and non-MVR (HR 2.70, 95% CI 1.09–6.56, $p = 0.032$).

Cumulative incidence of and risk factors for HCC development in patients with chronic hepatitis and cirrhosis

The results of univariate analysis with the log-rank test for the development of HCC in chronic hepatitis patients treated with LAM are shown in Table 4, and the following were significant risk factors: older age (≥50 years) ($p = 0.002$), HBe Ag negativity ($p = 0.005$), and low platelet count (<14 × 10^4/mm^3) ($p = 0.004$). Suppression of median HBV-DNA levels to <4.0 log copies/ml by LAM treatment was not associated with the development of HCC in the chronic hepatitis patients. Only non-MVR (median HBV-DNA amount ≥4.0 log copies/ml) was shown to be a significant risk factor for the development of HCC in the cirrhosis patients ($p = 0.029$), while the factors of age, HBe Ag status, and platelet count were not significant in these patients (Table 4).

Table 2 Risk factors for HCC development in all HBV-infected patients by univariate analysis

Factor	95% CI	*p* value
Age (years) (<50/≥50)	2.15–14.5	<0.001
Sex (male/female)	0.33–1.76	0.520
Initial diagnosis (chronic hepatitis/cirrhosis)	3.75–1.176	<0.001
HBe Ag (positive/negative)	0.31–1.29	0.209
HBV DNA (log copies/ml) (<7.0/>7.0)	0.33–1.35	0.262
AST (IU/l) (<40/≥40)	0.33–2.22	0.742
ALT (IU/l) (<40/≥40)	0.17–1.16	0.188
Total bilirubin (mg/dl) (<1.2/>1.2)	1.43–6.72	0.004
Alb (g/dl) (<3.8/≥3.8)	0.19–0.86	0.019
Platelets ($\times 10^4$/mm^3) (<14/≥14)	0.02–0.31	<0.001
Emergence of LAM-resistant viruses (positive/negative)	0.51–2.03	0.968
IVR (positive/negative)	0.52–3.25	0.575
MVR (positive/negative)	1.04–5.95	0.035

HCC Hepatocellular carcinoma, *HBV* hepatitis B virus, *CI* confidence interval, *HBe Ag* hepatitis B e antigen, *HBV* hepatitis B virus, *AST* aspartate aminotransferase, *ALT* alanine aminotransferase, *Alb* albumin, *IVR* initial viral response, *MVR* maintained viral response, *LAM* lamivudine

Table 3 Risk factors for HCC development in all HBV-infected patients by multivariate analysis

Factor	Category	Risk ratio	95% CI	*p* value
Age (years)	<50	1	1.08–9.53	0.036
	≥50	3.20		
Initial diagnosis	Chronic hepatitis	1	1.75–12.4	0.002
	Cirrhosis	4.64		
Platelets ($\times 10^4$/mm^8) (<14/≥14)	≥14	1	0.05–0.96	0.045
	<14	4.76		
MVR	Negative	1	1.09–6.56	0.032
	Positive	0.37		

HCC Hepatocellular carcinoma, *HBV* hepatitis B virus, *CI* confidence interval, *MVR* maintained viral response

Cumulative incidence of HCC development according to effectiveness of treatment (MVR vs. non-MVR)

Figure 2a shows the Kaplan–Meier curve of cumulative HCC incidence in all HBV-infected patients treated with LAM according to the effectiveness of treatment (MVR vs. non-MVR). The cumulative carcinogenesis rate for MVR-positive patients was 2% at 3 years, 4% at 5 years, and 6% at 7 years. On the other hand, the cumulative carcinogenesis rate for MVR-negative patients was 5% at 3 years, 13% at 5 years, and 16% at 7 years. MVR during LAM significantly suppressed the cumulative HCC incidence compared with non-MVR in all HBV-infected patients ($p = 0.035$).

Table 4 Risk factors for HCC development by univariate analysis (chronic hepatitis/cirrhosis)

	95% CI	*p* value
Chronic hepatitis		
Age (years) (<50/≥50)	0.26–8.38	0.002
Sex (male/female)	0.37–6.42	0.556
HBe Ag (positive/negative)	0.01–0.74	0.005
HBV DNA (log copies/ml) (<7.0/≥7.0)	0.11–1.99	0.296
AST (IU/l) (<40/≥40)	0.11–2.64	0.482
ALT (IU/l) (<40/≥40)	0.06–1.41	0.101
Total bilirubin (mg/dl) (<1.2/≥1.2)	0.67–6.67	0.574
Alb (g/dl) (<3.8/≥3.8)	0.13–8.58	0.960
Platelets ($\times 10^4$/mm^3) (<14/≥14)	0.01–0.72	0.004
Emergence of LAM-resistant viruses (positive/negative)	0.27–4.28	0.927
IVR (positive/negative)	0.29–8.67	0.590
MVR (positive/negative)	0.51–37.10	0.144
Cirrhosis		
Age (years) (<50/≥50)	0.86–6.17	0.089
Sex (male/female)	0.21–1.82	0.380
HBe Ag (positive/negative)	0.80–4.17	0.149
HBV DNA (log copies/ml) (<7.0/≥7.0)	0.40–2.01	0.795
AST (IU/l) (<40/≥40)	0.27–3.07	0.873
ALT (IU/l) (<40/≥40)	0.13–1.47	0.167
Total bilirubin (mg/dl) (<1.2/≥1.2)	0.82–4.80	0.126
Alb (g/dl) (<3.8/≥3.8)	0.28–1.58	0.354
Platelets ($\times 10^4$/mm^3) (<14/≥14)	0.03–1.51	0.084
Emergence of LAM-resistant viruses (positive/negative)	0.44–2.18	0.948
IVR (positive/negative)	0.90–8.32	0.063
MVR (positive/negative)	1.07–0.029	

HCC Hepatocellular carcinoma, *HBV* hepatitis B virus, *CI* confidence interval, *HBe Ag* hepatitis B e antigen, *HBV* hepatitis B virus, *AST* aspartate aminotransferase, *ALT* alanine aminotransferase, *Alb* albumin, *IVR* initial viral response, *MVR* maintained viral response

Figure 2b shows the Kaplan–Meier curve of the cumulative HCC incidence in chronic hepatitis patients according to the effectiveness of treatment (MVR vs. non-MVR). The cumulative carcinogenesis rate for MVR-positive patients was 0% at 3 years, 0% at 5 years, and 2% at 7 years. On the other hand, the cumulative carcinogenesis rate for MVR-negative patients was 2% at 3 years, 4% at 5 years, and 6% at 7 years. MVR during LAM did not significantly suppress the cumulative HCC incidence compared with non-MVR in the chronic hepatitis patients ($p = 0.144$).

Figure 2c shows the Kaplan–Meier curve of the cumulative HCC incidence in cirrhosis patients according to the effectiveness of treatment (MVR vs. non-MVR).

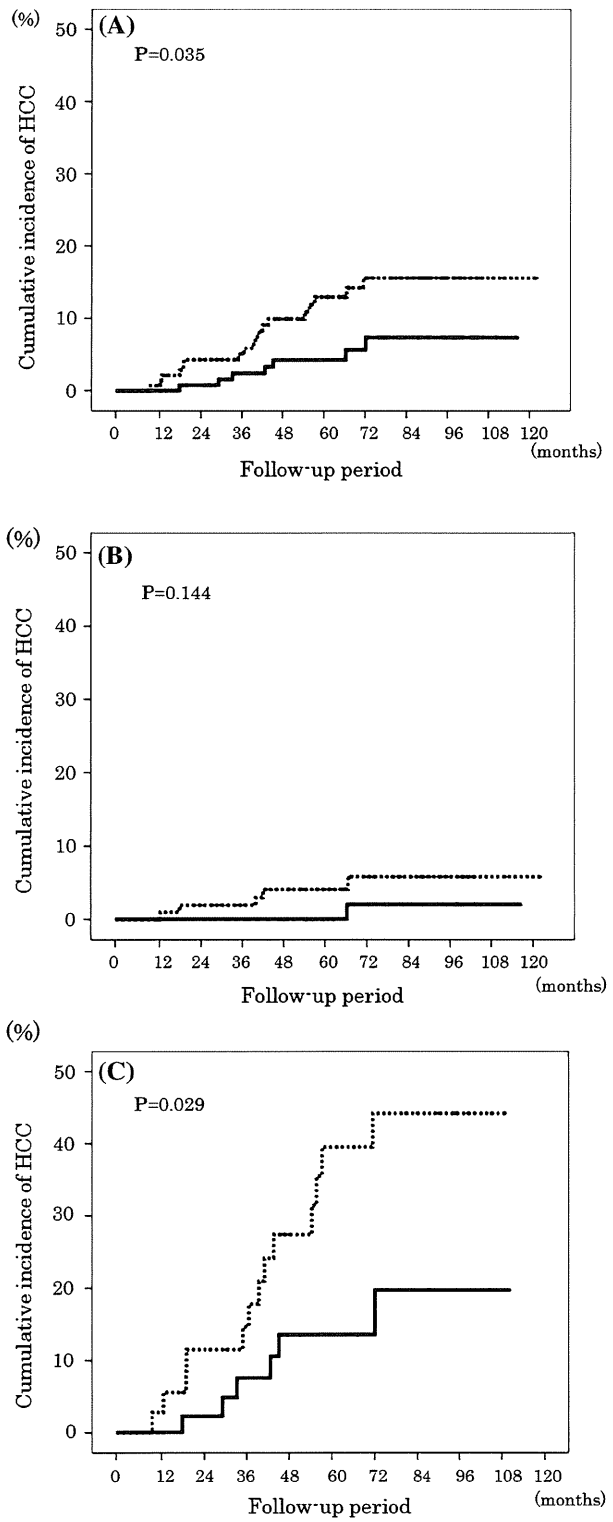

Fig. 2 Cumulative incidence of development of HCC according to the effectiveness of treatment (MVR vs. non-MVR). **a** All cases; **b** chronic hepatitis; **c** cirrhosis. *Solid lines* MVR, *dotted lines* non-MVR. *MVR* Maintained viral response

The cumulative carcinogenesis rate for MVR-positive patients was 8% at 3 years, 14% at 5 years, and 14% at 7 years. On the other hand, the cumulative carcinogenesis rate for MVR-negative patients was 18% at 3 years, 40% at 5 years, and 44% at 7 years. MVR during LAM significantly suppressed the cumulative HCC incidence compared with non-MVR in the cirrhosis patients ($p = 0.029$).

Relationship between IVR and MVR

Maintained viral response (MVR) was achieved by 142 (48%) of the 293 patients enrolled in this study. IVR was achieved by 204 (79%) of the 259 patients who were examined for IVR. The relationship between IVR and MVR is shown in Fig. 3; 60% (122/204) of the IVR-positive patients achieved an MVR, while only 16% (9/55) of the IVR-negative patients achieved an MVR ($p < 0.001$). The LAM-resistant YMDD mutant virus was found in 149 (51%) of all patients during follow-up, and in 52% (107/204) of the IVR-positive patients, a finding which was nearly equal to that for the IVR-negative patients (51%, 28/55). Among the IVR-positive patients, the MVR rate was lower in patients with the YMDD mutation, compared with that in those without the YMDD mutation (44%, 47/107 vs. 77%, 75/97, $p = 0.016$), while the MVR rates were low in the IVR-negative patients, irrespective of their YMDD mutation status (with and without the mutation, 15 vs. 18%, respectively). ADV was added to LAM treatment for 73 (68%) of the 107 IVR-positive patients with the YMDD mutation and 20 (36%) of the 55 IVR-negative patients with the YMDD mutation. However, MVR was only achieved at the low rates of 33% (24/73) for the former patients and 20% (4/20) for the latter.

Discussion

Lamivudine treatment has been shown to improve the liver histological findings in patients with HBV-infected liver disease by reducing the HBV load and stabilizing inflammatory activity [16–18]. One report has shown that LAM effectively reduced the incidence of HCC in patients with chronic hepatitis B, but the study only compared LAM-treated patients with non-treated patients in a matched case-controlled study [19]. However, there have been few detailed reports about the relationship between virological response and HCC development in HBV-infected patients during LAM treatment. In the present study, we retrospectively examined the incidence of HCC to clarify the indicators of LAM therapy, including median HBV-DNA levels, for reducing the risk of HCC in HBV-infected patients.

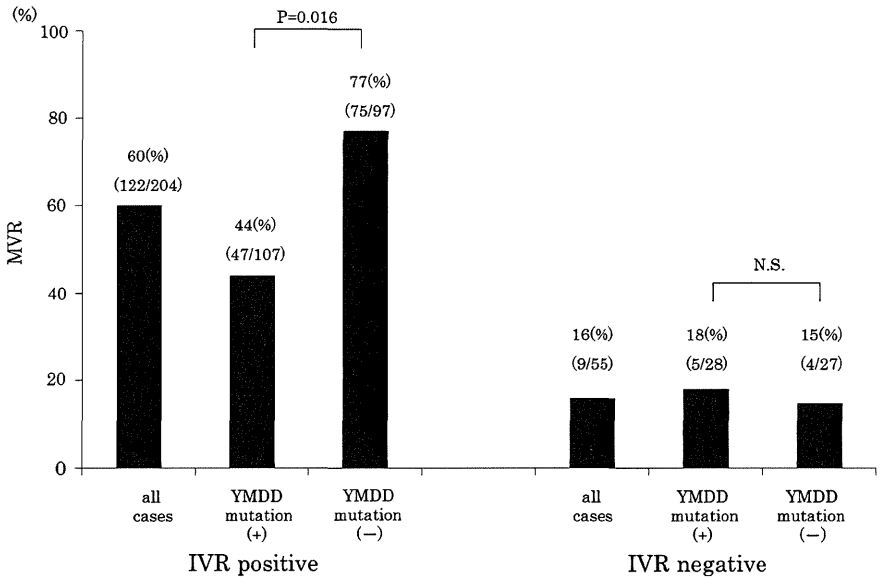

Fig. 3 Relationship between IVR and MVR. *IVR* Initial viral response, *MVR* maintained viral response, *N.S.* not significant

Many investigators have reported that serum HBV DNA levels higher than 4.0–4.5 log copies/ml before HBV treatment serve as a strong risk predictor of HCC [23–25]. Di Marco et al. [26] have reported that the incidence of HCC was higher in patients with serum HBV levels of more than 5.0 log copies/ml, at least once, during LAM therapy than in those in whom serum HBV levels were maintained at 5.0 log copies/ml or less. However, the add-on ADV therapy had not been adopted when the study of Di Marco et al. was reported. When the use of ADV is possible, an evaluation method is needed to measure the antiviral effects of nucleoside/nucleotide analogues against HBV-related liver disease. In the present study, we set the cut-off value for HBV-DNA at 4.0 log copies/ml. The basis of this cut-off value is that a serum HBV DNA level higher than 4.0 log copies/ml before HBV treatment was reported to serve as a strong risk predictor of HCC [23]. MVR, defined as a median HBV-DNA level of less than 4.0 log copies/ml measured every 6 months during therapy, was adopted as an indicator of viral replication, and non-MVR (median HBV-DNA >4.0 log copies/ml) during LAM therapy was shown to be significantly associated with the development of HCC in HBV-infected patients. We also found that a median HBV-DNA level of >4.0 log copies/ml during LAM therapy was a risk factor for HCC development. On the other hand, IVR, defined as HBV-DNA of <4.0 log copies/ml in the first 6 months of the follow-up period after the initiation of therapy, was not associated with the development of HCC in HBV patients in this study. As shown in Fig. 3, 84% of the IVR-negative patients could not achieve an MVR, suggesting that it is crucial to achieve an IVR in order to achieve an MVR. The reason why IVR was not a significant factor for MVR seemed to be the appearance of the YMDD mutation, which reduced the antiviral effect of LAM for HBV in IVR-positive patients. The LAM-resistant YMDD mutant virus was found in 52% of the IVR-positive patients. Although ADV was added to LAM treatment for 73 patients, only 33% of these patients could achieve an MVR. We speculate that the antiviral effect of ADV is not very strong [27] and it takes time to reduce the YMDD mutant virus, which may explain the low MVR rate (33%) in patients with the add-on ADV therapy. The immediate administration of ADV when the LAM-resistant YMDD mutant virus appears can be important [28]. A switch to ETV, which induces resistant virus less frequently, could also raise MVR rates among IVR-positive patients without the YMDD mutant virus.

As the duration of the add-on ADV therapy was included in this study, we compared the cumulative incidence of HCC in patients receiving LAM monotherapy with that in patients who also received the add-on ADV therapy. Sixteen (10%) of the 164 patients who received the LAM monotherapy developed HCC and the cumulative carcinogenesis rate was 6% at 3 years, 10% at 5 years, and 15% at 7 years. On the other hand, 16 (12%) of the 129 patients who received LAM plus ADV developed HCC and the cumulative carcinogenesis rate was 6% at 3 years, 12% at 5 years, and 14% at 7 years. No significant difference was found between these two groups ($p = 0.986$). In addition, we examined the cumulative incidence of HCC development according to the effectiveness of treatment (MVR vs. non-MVR) in patients for whom the observation period was terminated when ADV was added, and the same results were obtained (data not shown).

Older age (≥50 years), cirrhosis, and low platelet count ($<14 \times 10^4/mm^3$) were shown to be significantly associated with the development of HCC in patients with HBV infection. These results were consistent with those of

previous reports [29–31], suggesting that patients of older age with advanced fibrosis should be followed up carefully for longer periods in order to detect early stages of HCC even if LAM therapy does effectively suppress HBV. Of note, in the present study we estimated the cumulative HCC incidence according to the initial diagnosis of chronic hepatitis or cirrhosis. In the chronic hepatitis patients, older age (≥50 years), HBe Ag negativity, and low platelet count ($<14 \times 10^4/mm^3$) were significant risk factors for the development of HCC, but this was not the case in the cirrhosis patients. Because liver biopsies had not been performed, the liver fibrosis stage could not be evaluated with respect to the risk factors for HCC in this study. Instead, the factors of age, HBe Ag status, and platelet count may reflect the degree of liver fibrosis in chronic hepatitis patients. In fact, cirrhotic patients, in comparison with chronic hepatitis patients, were of older age (chronic hepatitis vs. cirrhosis: 46.3 ± 10.7 vs. 51.9 ± 9.8 years, $p < 0.001$), had higher rates of HBe Ag negativity (chronic hepatitis vs. cirrhosis: 39 vs. 51%, $p = 0.065$), and had lower platelet counts (chronic hepatitis vs. cirrhosis: 15.6 ± 4.9 vs. $9.3 \pm 3.8 \times 10^4/mm^3$, $p < 0.001$). This seems to explain why none of these factors were significant risk factors for HCC in cirrhotic patients. On the other hand, in the chronic hepatitis patients, MVR was not a significant factor for HCC development, while MVR was a significant factor for HCC development in the cirrhotic patients. We speculate that HBV suppression induced by LAM therapy could reduce the incidence of HCC in patients infected with HBV, especially those with cirrhosis, who displayed higher malignant potential. Investigation over a longer period is needed to clarify the effect of HBV suppression on the development of HCC in chronic hepatitis patients.

In conclusion, the present study shows that the attainment of an MVR induced by LAM therapy has a significant beneficial effect on the clinical course of HBV-infected patients by decreasing the incidence of HCC. The newer nucleotide analogues, such as ETV and tenofovir, should be able to further reduce the incidence of HCC, given their greater potency.

Acknowledgments This work was supported by Grants-in-Aid for Research on Hepatitis and BSE from the Ministry of Health Labour and Welfare of Japan and for Scientific Research from the Ministry of Education, Science, and Culture of Japan.

Conflict of interest The authors declare that they have no conflict of interest.

References

1. Lok AS, McMahon BJ. Chronic hepatitis B. Hepatology. 2007;45:507–39.
2. Lavanchy D. Hepatitis B virus epidemiology, disease burden, treatment, and current and emerging prevention and control measures. J Viral Hepat. 2004;11:97–107.
3. Lee WM. Hepatitis B virus infection. N Engl J Med. 1997;337:1733–45.
4. Beasley RP. Hepatitis B virus: the major etiology of hepatocellular carcinoma. Cancer. 1988;61:1942–56.
5. Lok SF. Chronic hepatitis B. N Engl J Med. 2002;346:1682–3.
6. Tang B, Kruger WD, Chen G, Shen F, Lin WY, Mboup S, et al. Hepatitis B viremia is associated with increased risk of hepatocellular carcinoma in chronic careers. J Med Virol. 2004;72:35–40.
7. Kim SR, Kudo M, Hino O, Han KH, Chung YH, Lee HS. Epidemiology of hepatocellular carcinoma in Japan and Korea. A review. Oncology. 2008;75:13–6.
8. Marcellin P, Chang TT, Lim SG, Tong MJ, Sievert W, Shiffman ML, et al. Adefovir dipivoxil for the treatment of hepatitis B e antigen-positive chronic hepatitis B. N Engl J Med. 2003;348:808–16.
9. Taura K, Ikai I, Hatano E, Fujii H, Uyama N, Shimahara Y. Implication of frequent local ablation therapy for intrahepatic recurrence in prolonged survival of patients with hepatocellular carcinoma undergoing hepatic resection: an analysis of 610 patients over 16 years old. Ann Surg. 2006;244:265–73.
10. Shimada K, Sano T, Sakamoto Y, Kosuge T. A long-term follow-up and management study of hepatocellular carcinoma patients surviving for 10 years or longer after curative hepatectomy. Cancer. 2005;104:1939–47.
11. Takayasu K, Arii S, Ikai I, Omata M, Okita K, Ichida T, et al. Prospective cohort study of transarterial chemoembolization for unresectable hepatocellular carcinoma in 8510 patients. Gastroenterology. 2006;131:461–9.
12. Dienstag JL, Perrillo RP, Schiff ER, Bartholomew M, Vicary C, Rubin M. A preliminary trial of lamivudine for chronic hepatitis B infection. N Engl J Med. 1995;333:1657–61.
13. Nevens F, Main J, Honkoop P, Tyrrell DL, Barber J, Sullivan MT, et al. Lamivudine therapy for chronic hepatitis B: a six-month randomized dose-ranging study. Gastroenterology. 1997;113:1258–63.
14. Rapti I, Dimou E, Mitsouka P, Hadziyannis SJ. Adding-on versus switching-to adefovir therapy in lamivudine-resistant HBVAg-negative chronic hepatitis B. Hepatology. 2007;45:307–13.
15. Chang TT, Lai CL, Kew Yoon S, Lee SS, Coelho HS, Carriho FJ, et al. Entecavir treatment for 5 years in patients with hepatitis Be antigen-positive chronic hepatitis B. Hepatology. 2010;51:422–30.
16. Kiyosawa K, Tanaka E, Sodeyama T. Hepatitis C virus and hepatocellular carcinoma. Curr Stud Hematol Blood Transfus. 1998;62:161–80.
17. Ohkoshi S, Norio O, Ichida T. The long-term clinical outcome of 1-year treatment of chronic hepatitis B with lamivudine-5 years observation. Hepatol Res. 2003;27:13–7.
18. Chu CM, Liaw YF. Hepatitis B virus-related cirrhosis: natural history and treatment. Semin Liver Dis. 2006;26:142–52.
19. Matsumoto A, Tanaka E, Rokuhara A, Kiyosawa K, Kumada H, Omata M, et al. Efficacy of lamivudine for preventing hepatocellular carcinoma in chronic hepatitis B: a multicenter retrospective study of 2795 patients. Hepatol Res. 2005;32:173–84.
20. Shamliyan TA, MacDonald R, Shaukat A, Taylor BC, Yuan JM, Johnson JR, et al. Antiviral therapy for adults with chronic hepatitis B: a systematic review for a National Institutes of Health Consensus Development Conference. Ann Intern Med. 2009;150(2):111–24.
21. Liaw YF, Sung JJ, Chow WC, Farrell G, Lee CZ, Yuen H, et al. Lamivudine for patients with chronic hepatitis B and advanced liver disease. N Engl J Med. 2004;351(15):1521–31.

22. Perrillo R, Hann HW, Mutimer D, Willems B, Leung N, Lee WM, et al. Adefovir dipivoxil added to ongoing lamivudine in chronic hepatitis B with YMDD mutant hepatitis B virus. Gastroenterology. 2004;126:81–90.
23. Chen CJ, Yang HI, Su J, Jen CL, You SL, Lu SN, et al. Risk of hepatocellular carcinoma across a biological gradient of serum hepatitis B virus DNA level. JAMA. 2006;295:65–73.
24. Chan HL, Hui AY, Wong ML, Tse AM, Hung LC, Wong VW, et al. Genotype C hepatitis B virus infection is associated with increased risk of hepatocellular carcinoma. Gut. 2004;53:1494–8.
25. Chan HL, Tse CH, Koh FM, Wong VW, Wong GL, Chan SL, et al. High viral load and hepatitis B virus subgenotype Ce are associated with increased risk of hepatocellular carcinoma. J Clin Oncol. 2008;26:177–82.
26. Di Marco V, Marzano A, Lampertico P, Andreone P, Santantonio T, Almasio PL, et al. Clinical outcome of HBeAg-negative chronic hepatitis B in relation to virological response to lamivudine. Hepatology. 2004;40:883–91.
27. Marcellin P, Chang TT, Lim SG, Tong MJ, Sievert W, Shiffman ML, et al. Adefovir dipivoxil for the treatment of hepatitis B e antigen-positive chronic hepatitis B. N Engl J Med. 2003;348:808–16.
28. Kurashige N, Hiramatsu N, Ohkawa K, Yakushijin T, Kiso S, Kanto T, et al. Factors contributing to antiviral effect of adefovir dipivoxil therapy added to ongoing lamivudine treatment in patients with lamivudine-resistant chronic hepatitis B. J Gastroenterol. 2009;44(6):601–7.
29. Chen CJ, Yu MW, Liaw YF. Epidemiological characteristics and risk factors of hepatocellular carcinoma. J Gastroenterol Hepatol. 1997;12:5294–308.
30. Yun LF. Natural history of chronic hepatitis B virus infection and long-term outcome under treatment. Liver Int. 2009;29:100–7.
31. Sung JJ, Tsoi KK, Wong VW, Li KC, Chan LL. Meta-analysis: treatment of hepatitis B infection reduces risk of hepatocellular carcinoma. Aliment Pharmacol Ther. 2008;28:1067–77.

Eur Radiol (2012) 22:845–854
DOI 10.1007/s00330-011-2316-y

HEPATOBILIARY-PANCREAS

Hypervascular hepatocellular carcinomas: detection with gadoxetate disodium-enhanced MR imaging and multiphasic multidetector CT

Hiromitsu Onishi · Tonsok Kim · Yasuharu Imai · Masatoshi Hori · Hiroaki Nagano · Yasuhiro Nakaya · Takahiro Tsuboyama · Atsushi Nakamoto · Mitsuaki Tatsumi · Seishi Kumano · Masahiro Okada · Manabu Takamura · Kenichi Wakasa · Noriyuki Tomiyama · Takamichi Murakami

Received: 4 July 2011 / Revised: 29 September 2011 / Accepted: 15 October 2011 / Published online: 7 November 2011

Abstract
Objectives To retrospectively compare the accuracy of detection of hypervascular hepatocellular carcinoma (HCC) by multiphasic multidetector CT and by gadoxetate disodium-enhanced MR imaging.
Methods After ethical approval, we analysed a total of 73 hypervascular HCC lesions from 31 patients suspected of having HCC, who underwent both gadoxetate disodium-enhanced MR imaging and multiphasic multidetector CT. Five blinded observers independently reviewed CT images, as well as dynamic MR images alone and combined with hepatobiliary phase MR images. Diagnostic accuracy (Az values), sensitivities and positive predictive values were compared by using the Scheffe post hoc test.
Results The mean Az value for dynamic and hepatobiliary phase MR combined (0.81) or dynamic MR images alone (0.78) was significantly higher than that for CT images (0.67, $P<0.001$, 0.005, respectively). The mean sensitivity of the combined MR images (0.67) was significantly higher than that of dynamic MR alone (0.52, $P<0.05$) or CT images (0.44, $P<0.05$). The mean positive predictive values were 0.96, 0.95 and 0.94, for CT, dynamic MR alone and combined MR images, respectively.
Conclusions Compared with multiphasic multidetector CT, gadoxetate disodium-enhanced MR imaging combining dynamic and hepatobiliary phase images results in significantly improved sensitivity and diagnostic accuracy for detection of hypervascular HCC.
Key Points
- *Gadoxetate disodium is a new liver-specific MR imaging contrast agent. Gadoxetate disodium-enhanced MRI helps the assessment of patients with liver disease.*
- *It showed high diagnostic accuracy for the detection of hepatocellular carcinoma.*

H. Onishi (✉) · T. Kim · M. Hori · Y. Nakaya · T. Tsuboyama · A. Nakamoto · M. Tatsumi · N. Tomiyama
Department of Radiology,
Osaka University Graduate School of Medicine,
2-2, Yamadaoka,
Suita, Osaka 565-0871, Japan
e-mail: h-onishi@iris.dti.ne.jp

Y. Imai
Department of Gastroenterology, Ikeda Municipal Hospital,
3-1-18, Johnan,
Ikeda, Osaka 563-8510, Japan

H. Nagano
Department of Surgery,
Osaka University Graduate School of Medicine,
2-2, Yamadaoka,
Suita, Osaka 565-0871, Japan

S. Kumano · M. Okada · T. Murakami
Department of Radiology, Kinki University School of Medicine,
377-2, Ohno-higashi,
Osakasayama, Osaka 589-8511, Japan

M. Takamura
Department of Radiology, Ikeda Municipal Hospital,
3-1-18, Johnan,
Ikeda, Osaka 563-8510, Japan

K. Wakasa
Department of Diagnostic Pathology,
Osaka City University Graduate School of Medicine,
1-4-3, Asahimachi, Abeno,
Osaka, Osaka 545-8585, Japan

Keywords Hepatocellular carcinoma · Magnetic resonance imaging · Computed tomography · Comparative study · Gadoxetate disodium

Introduction

Along with biopsy, diagnostic imaging such as multiphasic computed tomography (CT) or magnetic resonance (MR) imaging is reliably used for the assessment of hepatocellular carcinoma (HCC) [1–5]. According to the diagnostic algorithm suggested by the American Association for the Study of Liver Diseases (AASLD), a hepatic mass larger than 1 cm in diameter in a cirrhotic liver that demonstrates a typical vascular pattern (arterial hypervascularity and "washout" in the equilibrium phase) on CT or MR imaging can be diagnosed as HCC without biopsy [1, 2]. Evaluation of lesion vascularity (i.e. hypervascular or hypovascular) as well as detection of the focal lesion are thus essential elements of diagnosis of HCC through imaging.

Gadoxetate disodium (Primovist) is a liver-specific MR imaging contrast agent taken up by hepatocytes [6–12] and facilitates accurate detection of focal liver lesions on MR images during the hepatobiliary phase [13–21]. Several studies have compared gadoxetate disodium-enhanced MR imaging with multiphasic multidetector CT for the detection of HCC [22–24]. To the best of our knowledge, however, the literature contains no comparative study of the diagnostic accuracy for the detection of hypervascular HCC which is also based on careful evaluation of tumour vascularity. Use of gadoxetate disodium produces not only liver-specific hepatobiliary but also dynamic MR images, which makes it possible to evaluate tumour vascularity [22–30]. However, since the amount of gadolinium in gadoxetate disodium medium (0.025 mmol/kg) is smaller than that in extracellular gadolinium chelates medium (0.1 mmol/kg) at the recommended dosage, dynamic MR imaging using gadoxetate disodium could impair tumour enhancement in the arterial dominant phase [31] and compromise characterisation of the lesions based on vascularity.

The purpose of our study was to retrospectively compare the accuracy for detection of hypervascular HCC by means of multiphasic multidetector CT and gadoxetate disodium-enhanced MR imaging.

Materials and methods

This retrospective study was implemented at three institutions (Osaka University Hospital, Kinki University Hospital, and Ikeda Municipal Hospital) and approved, with waiver of informed consent, by the ethics committee of each institution.

Patient population

Ninety-seven consecutive patients with chronic liver disease and suspected of having HCC, who underwent both multiphasic multidetector CT and gadoxetate disodium-enhanced MR imaging within a 6-week period between March and December, 2008, were eligible for the study. However, 66 (68%) of these patients were excluded from the study population because no angio-CT including double-phase CT during hepatic arteriography (CTHA) nor CT during arterial portography (CTAP) was performed (n=61), or because of inadequate MR examination (n=5). The remaining 31 patients (28 men and 3 women; mean age, 70.2 years; range, 52–82 years) constituted the study population (Fig. 1). Four of them had hepatitis B, 21 had hepatitis C, four had alcohol-related hepatitis and one had nonalcoholic steatohepatitis. Total bilirubin values of these patients ranged from 0.4 to 2.2 mg/dL (mean, 1.0 mg/dL). Twenty-three patients were classified as Child-Pugh A, and the remaining eight patients were classified as Child-Pugh B.

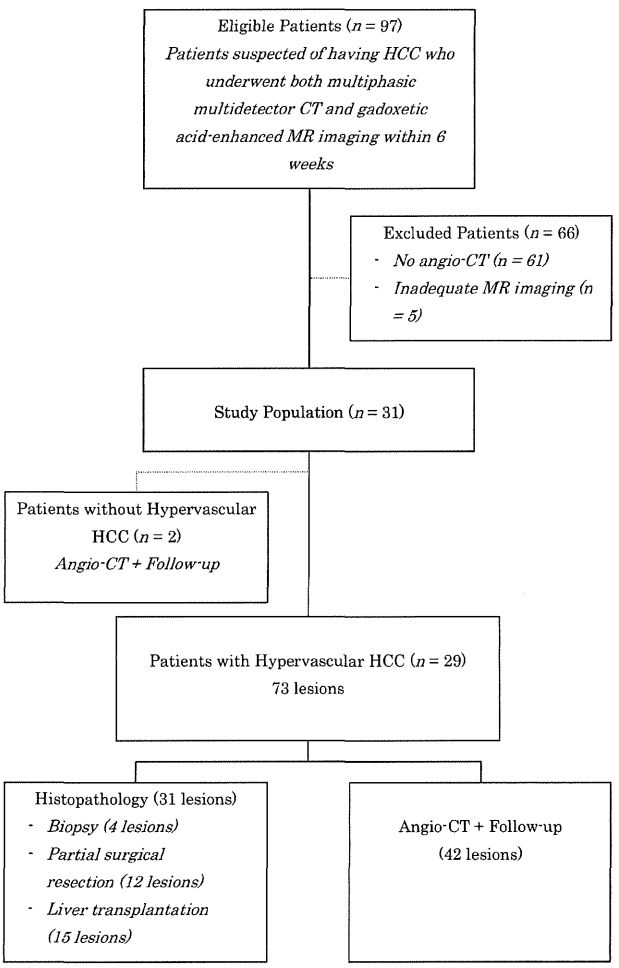

Fig. 1 Flowchart of patient enrollment and proof of tumour burden

Twenty-five of the patients underwent multidetector CT before MR imaging, and the mean interval between CT and MR imaging was 19 days.

Proof of tumour burden

Of the 31 patients evaluated, 29 had a total of 73 confirmed hypervascular HCC nodules. The nodules ranged from 0.3 to 14 cm in diameter (mean, 1.8 cm). While 31 HCC nodules were diagnosed histologically (partial surgical resection, n=12; biopsy, n=4; liver transplantation, n=15), the remaining 42 hypervascular HCCs were diagnosed clinically on the basis of tumour markers, double-phase CTHA and CTAP [32], follow-up CT and/or MR imaging (mean follow-up, 19 months; range 4–26 months). Whether the HCC nodules were of the arterial hypervascular or arterial hypovascular type was determined on the basis of the CTHA findings. Two patients had no hypervascular HCCs.

Multiphasic multidetector CT

Multiphasic CT was performed by using an 8-channel CT (n=9) (LightSpeed Ultra; GE Healthcare, Milwaukee, WI) or 64-channel CT (n=22) (LightSpeed VCT; GE Healthcare). The X-ray tube voltage was 120 kVp and the tube current was modulated automatically according to the patient's body size by means of an automatic tube current modulation technique (3D AutomA; GE Healthcare). The section thickness was 5 mm. All patients were given 2.0 mL (600 mg of iodine) per kilogram of body weight, with a maximum dose of 150 mL per patient, and 300 mgI/mL of the nonionic contrast medium. The warmed contrast medium was administered intravenously with a mechanical power injector at 3–5 mL/s with a fixed injection duration of 30 s through a 20-gauge catheter inserted into an arm vein. Multiphasic CT was performed immediately before contrast-medium administration and during the hepatic arterial dominant, portal venous dominant and equilibrium phases 30–45, 65–80, and 190–205 s, respectively, after the start of the contrast material injection [22–24, 33–35]. To determine the acquisition delay for hepatic arterial dominant phase imaging, a semiautomatic bolus-tracking technique was used (SmartPrep; GE Healthcare). Arterial dominant phase acquisition was started 22 s after the trigger threshold (50HU elevation) was reached at the suprarenal abdominal aorta.

MR imaging

MR imaging was performed with a 1.5-T system (n=23) (Signa Excite HD 1.5T; GE Healthcare, or Intera; Philips Medical Systems, Eindhoven, The Netherlands) or 3.0-T system (n=8) (Signa HD 3.0T; GE Healthcare) with body-array coils. For the contrast enhancement, 0.1 mL/kg (0.025 mmol/kg) of gadoxetate disodium (Primovist; Bayer-Schering Pharma AG, Berlin, Germany) diluted with saline to 10 mL (e.g. a patient with a body weight of 60 kg received 6 mL of gadoxetate disodium medium diluted with 4 mL of saline) was administered intravenously with a mechanical power injector at 1 mL/s with a fixed injection duration of 10 s through a 22-gauge catheter inserted into an arm vein, followed by a 30-mL saline flush at 1 mL/s. However, the maximum applied dose of gadoxetate disodium was 10 mL (2.5 mmol).

For MR imaging, in-phase and out-of-phase T1-weighted images, T2-weighted images, gadoxetate disodium-enhanced dynamic images (precontrast, arterial, and portal venous dominant phase), and hepatobiliary phase images (20 min after the injection) were acquired. Acquisition parameters are listed in Table 1. Gadoxetate disodium-enhanced dynamic imaging was performed with three-dimensional gradient-echo sequences (LAVA; GE Healthcare or THRIVE; Philips Medical Systems), and performed immediately before contrast-medium administration and during the hepatic arterial dominant and portal venous dominant phases 25–40 and 70 s, respectively, after the start of the contrast material injection. To determine the acquisition delay for hepatic arterial dominant phase imaging, the bolus tracking technique was used. Arterial dominant phase acquisition was started 15 s after the trigger point was reached at the suprarenal abdominal aorta.

Table 1 MR imaging sequences and parameters

Acquisition	Sequence	TR (ms)	TE (ms)	ETL	Flip angle (degrees)	FOV (mm)	Matrix	Thickness (mm)	Fat suppression
T1 in-phase	2D GRE	175–220	4.4 (5.8)	–	12	340×340	192×320	5	Not used
T1 out-of-phase	2D GRE	175–220	2.2 (2.6)	–	12	340×340	192×320	5	Not used
T2-w.i.	2D FSE	6666–10000	89–93	8	90	340×340	160×512	5	Used
Dynamic & HB	3D GRE (LAVA or THRIVE)	4.5–4.8	2.2–2.3	–	12	340×340	192×320	4	Used

Numbers in parentheses show parameters at 3.0T. *TR* repetition time, *TE* echo time, *ETL* echo train length, *FOV* field of view, *w.i.* weighted image, *3D* three-dimensional, *GRE* gradient echo, *2D* two-dimensional, *FSE* fast spin echo, *HB* hepatobiliary phase image, *LAVA* liver acquisition with volume acceleration, *THRIVE* T1 high-resolution isotropic volume excitation

Table 2 Az values for the detection of hypervascular HCC

	Reader 1	Reader 2	Reader 3	Reader 4	Reader 5	Mean
All lesions (n=73)						
Multiphasic CT	0.68	0.68	0.69	0.62	0.70	0.67*†
Dynamic MR imaging	0.78	0.73	0.80	0.78	0.83	0.78*
Combined dynamic and hepatobiliary phase MR imaging	0.84	0.74	0.80	0.82	0.86	0.81†
Lesions <1.0 cm (n=28)						
Multiphasic CT	0.55	0.60	0.50	0.46	0.57	0.53‡§
Dynamic MR imaging	0.78	0.72	0.82	0.79	0.82	0.79‡
Combined dynamic and hepatobiliary phase MR imaging	0.79	0.77	0.80	0.78	0.84	0.80§
Lesions 1.0–2.0 cm (n=32)						
Multiphasic CT	0.89	0.89	0.86	0.83	0.88	0.87
Dynamic MR imaging	0.86	0.72	0.80	0.79	0.90	0.81
Combined dynamic and hepatobiliary phase MR imaging	0.93	0.79	0.84	0.86	DD	0.85
Lesions >2.0 cm (n=13)						
Multiphasic CT	DD	DD	DD	DD	DD	N/A
Dynamic MR imaging	DD	DD	DD	DD	DD	N/A
Combined dynamic and hepatobiliary phase MR imaging	DD	DD	0.99	DD	DD	0.99

DD degenerate data. *CT vs. dynamic MR: P<0.01, †CT vs. combined MR: P<0.001, ‡CT vs. dynamic MR: P<0.001, §CT vs. combined MR: P<0.001, and there were no statistically significant differences at other pairings among the three imaging techniques. (Scheffe post-hoc multiple comparison)

Qualitative image analysis

For each patient, multiphasic multidetector CT images, gadoxetate disodium-enhanced dynamic MR images with T1- and T2-weighted images, and all MR images including hepatobiliary phase images were evaluated independently and blindly by five radiologists (readers 1, 2, 3, 4, and 5, with 19, 16, 8, 6, and 6 years experience, respectively, in gastrointestinal and hepatobiliary imaging). The images were read on a commercially available workstation. During one session,

Table 3 Sensitivity in the detection of hypervascular HCC

	Reader 1	Reader 2	Reader 3	Reader 4	Reader 5	Mean
All lesions (n=73)						
Multiphasic CT	0.37 (27)	0.40 (29)	0.53 (39)	0.36 (26)	0.56 (41)	0.44*
Dynamic MR imaging	0.41 (30)	0.53 (39)	0.60 (44)	0.45 (33)	0.59 (43)	0.52†
Combined dynamic and hepatobiliary phase MR imaging	0.67 (49)	0.63 (46)	0.63 (46)	0.71 (52)	0.73 (53)	0.67*†
Lesions <1.0 cm (n=28)						
Multiphasic CT	0.07 (2)	0.07 (2)	0.18 (5)	0.00 (0)	0.21 (6)	0.11‡
Dynamic MR imaging	0.11 (3)	0.29 (8)	0.36 (10)	0.14 (4)	0.29 (8)	0.24§
Combined dynamic and hepatobiliary phase MR imaging	0.46 (13)	0.43 (12)	0.43 (12)	0.57 (16)	0.50 (14)	0.48‡§
Lesions 1.0–2.0 cm (n=32)						
Multiphasic CT	0.44 (14)	0.50 (16)	0.72 (23)	0.47 (15)	0.75 (24)	0.58
Dynamic MR imaging	0.47 (15)	0.59 (19)	0.69 (22)	0.56 (18)	0.72 (23)	0.61
Combined dynamic and hepatobiliary phase MR imaging	0.72 (23)	0.69 (22)	0.69 (22)	0.81 (26)	0.84 (27)	0.75
Lesions >2.0 cm (n=13)						
Multiphasic CT	0.85 (11)	0.85 (11)	0.85 (11)	0.85 (11)	0.85 (11)	0.85
Dynamic MR imaging	0.85 (11)	0.92 (12)	0.92 (12)	0.69 (9)	0.92 (12)	0.86
Combined dynamic and hepatobiliary phase MR imaging	1.00 (13)	0.92 (12)	0.92 (12)	0.77 (10)	0.92 (12)	0.91

Numbers in parentheses are actual numbers of lesions. * CT vs. combined MR: P<0.01, †dynamic MR vs. combined MR: P<0.05, ‡CT vs. combined MR: P<0.001, §dynamic MR vs. combined MR: P<0.01, and there were no statistically significant differences at other pairings among the three imaging techniques. (Scheffe post-hoc multiple comparison)

image sets consisting of a mixture of MR images of half of the patients and CT images of the other half were presented in random order. During the other session, the remaining image sets were presented in random order. To minimise recall bias, each reading session was separated by at least 4 weeks.

Before the first reading session, the following criteria for diagnosing hypervascular HCC were provided to the readers: a) hyperenhancement during the hepatic arterial dominant phase; b) hypoattenuation or hypointensity compared with the surrounding liver during the portal venous or equilibrium phases (i.e. washout); c) hypointensity during the hepatobiliary phase; d) inhomogeneous isointensity or hyperintensity during the hepatobiliary phase [28, 33, 36, 37] and e) fat component in the nodule (lower attenuation than water on unenhanced CT images or signal reduction in the out-of-phase T1-weighted MR images in comparison with in-phase images). Hypervascular HCC was unequivocally diagnosed if a lesion fulfilled criterion (a) and any one of the other criteria (b–e). In addition, criteria for suspected but non-conclusive diagnosis of hypervascular HCC included f) mild hyperintensity on T2-weighted MR images with early enhancement or g) nodular arterial enhancement without washout. Hemangioma was differentiated from HCC on the basis of the following image findings: a) a globular enhancement pattern during the hepatic arterial dominant phase, b) prolonged enhancement during the portal venous or equilibrium phases on CT images and c) significant hyperintensity on T2-weighted MR images.

Each reader classified all detected lesions according to the following four-point confidence score scale: 1- probably no mass lesion present; 2- indefinite presence of lesion; 3- lesion probably present; and 4- definite presence of a lesion; with confidence scores of 3 and 4 representing a positive diagnosis of liver mass lesion. For evaluation of MR images, the readers, after reading the dynamic MR images with T1- and T2-weighted images and recording the decisions for a given patient, then examined the hepatobiliary phase images for the same patient and also recorded the decisions they made on the basis of all MR images.

Statistical analysis

For assessment of inter-reader variability for image interpretation, the unweighted κ statistic was used to measure

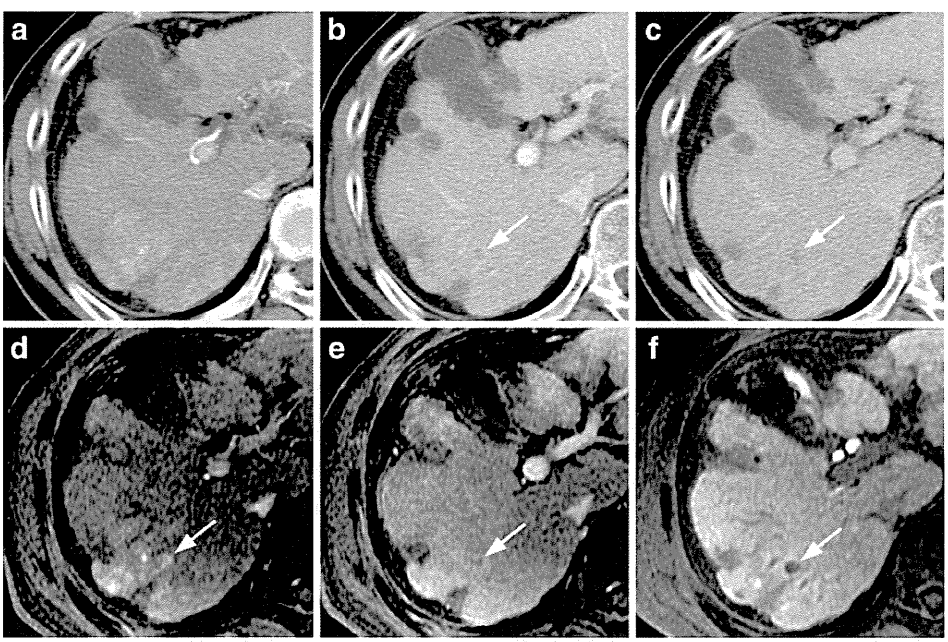

Fig. 2 HCC of a 60-year-old-man with hepatitis C cirrhosis, histologically proved at liver transplantation. CTHA revealed hypervascularity of the lesion (not shown). Contrast-enhanced CT image obtained during arterial dominant phase (**a**) does not show a hypervascular lesion in the right liver lobe, but images obtained during portal venous dominant (**b**) and equilibrium (**c**) phases show a nodule (*arrows*) with mild hypoattenuation compared with the surrounding liver parenchyma. Corresponding gadoxetic acid-enhanced MR image obtained during the arterial dominant (**d**) and portal venous dominant (**e**) phases show an 8-mm hypervascular nodule, which has become slightly hypoattenuating (*arrows*). On the MR image obtained during the hepatobiliary phase (20 min after contrast medium administration), the lesion has become hypointense against the highly enhanced background liver parenchyma (**f**). All the readers assigned this lesion a confidence score of 0 on CT images because of a lack of arterial hypervascularity. On dynamic MR images alone, two readers assigned it a score of 2, one assigned it a score of 3, and the remaining two readers assigned it a score of 4. On combined dynamic and hepatobiliary phase MR images, one reader assigned the lesion a score of 3, while the remaining four readers assigned it a score of 4. The addition of the hepatobiliary phase to dynamic MR images increased the confidence level for this lesion, because the lesion was conspicuously delineated on the hepatobiliary phase images

the extent of agreement among the five readers regarding the presence (score 3 or 4) or absence (score 2 or less) of lesions. κ values of up to 0.40 were considered to indicate positive but poor agreement; 0.41–0.75, good agreement; and 0.75 or higher, excellent agreement [38].

Alternative free-response receiver operating characteristic (AFROC) analysis (ROCKIT 0.9B; C. E. Metz, University of Chicago, Chicago, IL, USA) was performed on a tumour-by-tumour basis [39]. The area under each AFROC curve, that is, the Az value, was used to indicate the overall diagnostic performance of each technique and each reader.

Sensitivity and positive predictive values for lesion detection with each technique for each reader were also determined by using only lesions assigned a confidence rating of 3 or 4.

Mean Az values, mean sensitivities and mean positive predictive values were compared among the various techniques by using the Scheffe post hoc test. Statistical analyses were performed for all lesions and for the subgroups of lesions with maximum diameters of less than 1 cm, 1–2 cm, and more than 2 cm. A P value of less than 0.05 was considered to indicate a statistically significant difference.

Results

Inter-reader agreement

The κ values for the five readers were 0.70 for multiphasic multidetector CT, 0.54 for dynamic MR imaging, and 0.55 for combined dynamic and hepatobiliary phase MR imaging. As for the presence of lesions, good agreement among the five readers was obtained for the detection of hypervascular HCC lesions with each of the techniques.

AFROC analysis

For all hypervascular HCC lesions and the subgroup of lesions 1 cm in diameter or smaller, the mean Az value, or diagnostic accuracy, for dynamic MR imaging alone or combined dynamic and hepatobiliary MR imaging was significantly higher than that for multiphasic multidetector CT (Table 2). For the subgroup of lesions 1–2 cm in diameter, there was no statistically significant difference among the techniques. In most instances, the Az value for the subgroup of lesions larger than 2 cm was degenerated because it was based on a data set with many tied values.

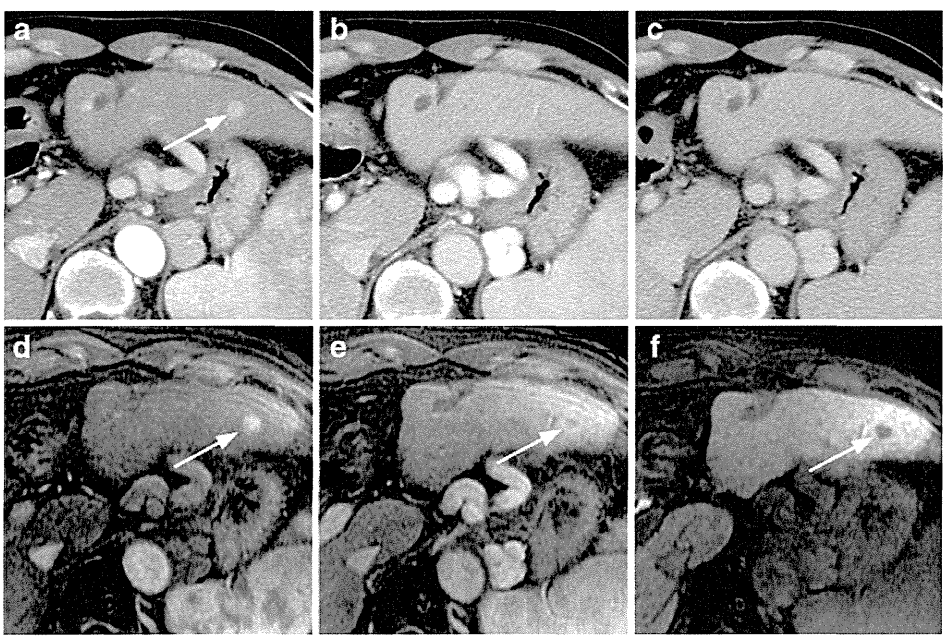

Fig. 3 Histologically proved HCC of a same patient as in Fig. 2. CTHA revealed hypervascularity of the lesion (not shown). Contrast-enhanced CT image obtained during the arterial dominant phase (**a**) shows a 10-mm hypervascular lesion in the left liver lobe (*arrow*), and images obtained during the portal venous dominant (**b**) and equilibrium (**c**) phases show isoattenuation compared with the surrounding liver parenchyma. The corresponding gadoxetic acid-enhanced MR images obtained during the arterial dominant (**d**) and portal venous dominant (**e**) phases show a hypervascular nodule, which has become slightly hypoattenuating (*arrows*). On the MR image obtained during the hepatobiliary phase (20 min after contrast medium administration), the lesion has become hypointense against the highly enhanced background liver parenchyma (**f**). On dynamic MR images alone, three readers assigned the lesion a score of 2, one assigned it a score of 3 and one assigned it a score of 4. On combined dynamic and hepatobiliary phase MR images, three readers assigned the lesion a score of 3 and the remaining two readers a score of 4. On CT images, three readers assigned this lesion a confidence score of 2 because of a lack of "washout" enhancement pattern and the other two assigned it a confidence score of 3

Sensitivity

For all hypervascular HCC lesions and the subgroup of lesions 1 cm in diameter or smaller, the mean sensitivity for combined dynamic and hepatobiliary MR imaging was significantly higher than that for multiphasic multidetector CT or dynamic MR imaging alone (Table 3, Fig. 2). For the subgroup of lesions 1–2 cm and 2 cm or more in diameter, the mean sensitivity for combined dynamic and hepatobiliary MR imaging was higher than that for multiphasic multidetector CT or dynamic MR imaging alone, although the difference was not statistically significant (Fig. 3).

Four of the 73 lesions showed hyperintensity in comparison with the surrounding liver parenchyma on the hepatobiliary phase MR images. Another three lesions in three patients showed isointensity at the hepatobiliary phase and in two of these patients, the liver parenchyma demonstrated minimal enhancement at the hepatobiliary phase due to deterioration of liver function.

False–negative findings

Eight lesions (all ≤1 cm) of five patients, which were confirmed during hepatic transplantation (n=3) or angio-CT with imaging follow-up (n=5), were not detected with a high confidence score of 3 or 4 by any of the readers on any of the image sets.

In terms of specific image sets, 30 lesions (>2 cm, n=2; 1–2 cm, n=7; <1 cm, n=21) in 12 patients were not detected on CT images with high confidence by any of the readers. Of these 30 lesions, 13 (>2 cm, n=2; 1–2 cm, n=4; <1 cm, n=7) in six patients were detected on dynamic MR images by at least one reader, while another nine lesions (1–2 cm, n=2; <1 cm, n=7) in eight patients were detected when hepatobiliary phase MR images were added to the dynamic MR images.

On gadoxetate disodium-enhanced dynamic MR images, 19 lesions (1–2 cm, n=5; <1 cm, n=14) in 10 patients were not detected with high confidence by any of the readers. Of these 19 lesions, nine (1–2 cm, n=2; <1 cm, n=7) in eight patients were detected when hepatobiliary phase MR images were added to the dynamic MR images and two lesions (1 cm, n=2) in two patients, which were not detected with combined dynamic and hepatobiliary phase MR images, were detected on CT images by at least one reader.

On combined dynamic and hepatobiliary phase MR images, eleven lesions (1–2 cm, n=3; <1 cm, n=8) in five patients were not detected with high confidence by any of the readers.

False-positive findings and positive predictive value

There were no significant differences between the mean positive predictive values for all three techniques (Table 4).

The false–positive lesions rated on CT images were retrospectively determined to be two arterial enhancing pseudolesion such as arterial-portal venous shunts (Fig. 4) and a regenerative nodule with mild atypia (histopathologically proven by biopsy). The actual numbers of false–positive lesions were 1, 1, 1, 1 and 2 for each reader, respectively, on CT images.

Table 4 Positive predictive values in the detection of hypervascular HCC

	Reader 1	Reader 2	Reader 3	Reader 4	Reader 5	Mean
All lesions (n=73)						
Multiphasic CT	0.96 (27/28)	0.97 (29/30)	0.98 (39/40)	0.96 (26/27)	0.95 (41/43)	0.96
Dynamic MR imaging	0.91 (30/33)	0.95 (39/41)	0.94 (44/47)	0.97 (33/34)	0.98 (43/44)	0.95
Combined dynamic and hepatobiliary phase MR imaging	0.94 (49/52)	0.88 (46/52)	0.94 (46/49)	0.98 (52/53)	0.93 (53/57)	0.94
Lesions <1.0 cm (n=28)						
Multiphasic CT	0.67 (2/3)	1.00 (2/2)	1.00 (5/5)	N/A (0/0)	0.86 (6/7)	0.88
Dynamic MR imaging	0.75 (3/4)	1.00 (8/8)	1.00 (10/10)	1.00 (4/4)	1.00 (8/8)	0.95
Combined dynamic and hepatobiliary phase MR imaging	0.93 (13/14)	0.75 (12/16)	1.00 (12/12)	1.00 (16/16)	0.88 (14/16)	0.91
Lesions 1.0–2.0 cm (n=32)						
Multiphasic CT	1.00 (14/14)	0.94 (16/17)	0.96 (23/24)	0.94 (15/16)	0.96 (24/25)	0.96
Dynamic MR imaging	0.88 (15/17)	0.90 (19/21)	0.92 (22/24)	0.95 (18/19)	0.96 (23/24)	0.92
Combined dynamic and hepatobiliary phase MR imaging	0.92 (23/25)	0.92 (22/24)	0.92 (22/24)	0.96 (26/27)	0.93 (27/29)	0.93
Lesions >2.0 cm (n=13)						
Multiphasic CT	1.00 (11/11)	1.00 (11/11)	1.00 (11/11)	1.00 (11/11)	1.00 (11/11)	1.00
Dynamic MR imaging	1.00 (11/11)	1.00 (12/12)	0.92 (12/13)	1.00 (9/9)	1.00 (12/12)	0.98
Combined dynamic and hepatobiliary phase MR imaging	1.00 (13/13)	1.00 (12/12)	0.92 (12/13)	1.00 (10/10)	1.00 (12/12)	0.98

Numbers in parentheses are actual numbers of lesions. Regardless of lesion size, there were no statistically significant differences among the imaging techniques

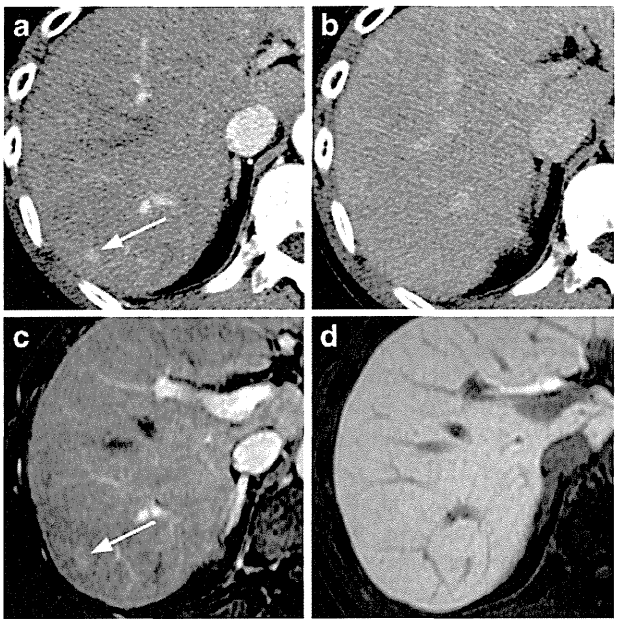

Fig. 4 Images of hepatitis B cirrhosis in a 68-year-old-man. Contrast-enhanced CT image obtained during the arterial dominant phase (**a**) shows a mildly enhanced lesion, 8 mm in diameter, in the right liver lobe (*arrow*), which has become isoattenuating during the equilibrium phase compared with the surrounding liver parenchyma (**b**). Corresponding gadoxetic acid-enhanced MR image obtained during the arterial dominant phase (**c**) shows a lesion 8 mm in diameter with slight enhancement (*arrow*). The MR image obtained during the hepatobiliary phase (20 min after contrast-medium administration), shows that the lesion has becomes isointense compared with the surrounding liver parenchyma (**d**). On CT images, one reader assigned this lesion a confidence score of 0, one assigned it a score of 1, two assigned it a score of 2 and one a score of 4. On both dynamic MR images alone and combined dynamic and hepatobiliary phase MR images, all the readers assigned it a score of 0. On CTAP images, this lesion did not show a perfusion defect, and on follow-up CT images obtained 3 months later, the hyperattenuation observed during the arterial dominant phase was not seen. This lesion was therefore considered to be an arterial enhancing pseudolesion

The false–positive lesions rated on dynamic MR images alone and on combined dynamic and hepatobiliary phase MR images were retrospectively determined to be five small arterial enhancing pseudolesion, fibrotic change, and a regenerative nodule with mild atypia. Additionally, two small hepatic hemangiomas were assigned a score of 3 by one or two readers on combined dynamic and hepatobiliary phase MR images. The actual numbers of false–positive lesions were 3, 2, 3, 1 and 1 on dynamic MR images alone and 3, 6, 3, 1 and 4 on combined dynamic and hepatobiliary phase MR images.

Discussion

Previous studies [23, 24] have reported that gadoxetate disodium-enhanced MR imaging and multiphasic multidetector CT produce a similar diagnostic performance (Az) for the detection of HCC using AFROC analysis. Our study demonstrated that, compared with multiphasic multidetector CT, gadoxetate disodium-enhanced MR imaging including dynamic and hepatobiliary phase imaging significantly improved not only the sensitivity but also the diagnostic accuracy for the detection of hypervascular HCC. One of the reasons for this difference may be that the size of the tumours examined in our study was smaller than that of tumours examined in previous studies. Statistical analyses of the subgroups classified by lesion size showed that only for the subgroup of lesions 1 cm in diameter or smaller, the mean Az for combined dynamic and hepatobiliary MR imaging was significantly higher than that for multiphasic multidetector CT. Meanwhile, there were no significant differences among the techniques in the detection lesions 1 cm in diameter or larger.

Since, at the recommended dosage, the amount of gadolinium in gadoxetate acid disodium medium is only one-fourth that in conventional extracellular gadolinium chelates medium, dynamic MR imaging using gadoxetate acid may show weaker enhancement than that using extracellular medium [31]. This might impair the sensitivity for detection of hypervascular HCC due to weaker tumour enhancement at the arterial dominant phase or compromise the characterisation of the lesions based on lesion vascularity. However, our study, which evaluated the diagnostic accuracy of HCC by taking tumour vascularity into consideration, demonstrated that sensitivity for the detection of hypervascular HCC on gadoxetate disodium-enhanced dynamic MR images without hepatobiliary images was higher than that for multiphasic multidetector CT, although the difference was not statistically significant, and that the diagnostic accuracy (Az) of gadoxetate disodium-enhanced dynamic MR imaging was significantly higher than that of CT. The use for dynamic imaging of a three-dimensional gradient-echo sequence dedicated to liver imaging (e.g. LAVA or THRIVE) may enhance MR imaging.

The addition of hepatobiliary phase images to dynamic images improved sensitivity for the detection of hypervascular HCC. However, more false–positive findings were identified on combined dynamic and hepatobiliary phase MR images than on dynamic images. Two small hemangiomas and an arterial enhancing pseudolesion were additionally classified as hypervascular HCCs by one or two readers on combined MR images. A previous study reported that high-flow hepatic hemangioma on gadoxetate disodium-enhanced MR imaging mimicked hypervascular tumour due to "pseudo washout" sign [40]. Another study reported that a small proportion of arterial enhancing pseudolesions demonstrated low signal intensity on hepatobiliary phase [41]. This may also result in the false–positive lesions.

Analyses of inter-reader variability demonstrated slightly lower agreement at MR imaging (both dynamic and combined images) compared to that at CT, although good agreement was obtained with each technique. This may be thought to be causally related to the complexity of diagnosis using various image contrasts and extended criteria for diagnosing HCC at MR imaging.

The present study has certain limitations. First, our study is a retrospective study and our study population was not a surveillance population. All patients were suspected of having at least one possible HCC nodule and underwent CT arterial portography, CT hepatic arteriography for trans-arterial chemoembolisation or evaluation before surgical resection. Selection bias may have resulted in an overestimation of the actual diagnostic performance because of the exclusion of negative imaging studies. Secondly, as in the case with some previous studies [22, 24, 42], a potential limitation of our study could be the lack of histologic proof for some HCCs. However, several kinds of confirmatory findings were available, including those obtained with CTAP, CTHA and follow-up CT or follow-up MR imaging. Thirdly, our study population size of 31 was rather small, so that, with a larger patient population, our data could have achieved more robust statistical significance. inally, at CT examination, an 8-channel CT was used for some patients; the use of 64-channel CT for these patients may improve the diagnostic performance at CT.

In summary, our results demonstrate that, compared with multiphasic multidetector CT, gadoxetate disodium-enhanced MR imaging including dynamic and hepatobiliary phase images results in significantly improved sensitivity and diagnostic accuracy for the detection of hypervascular HCC.

Acknowledgements This work was supported in part by a Grant-in-Aid for Young Scientists (21791191) from the Ministry of Education, Culture, Sports, Science and Technology and by Health and Labor Sciences Research Grants (KAKENHI), Japan Society for the Promotion of Science.

References

1. Bruix J, Sherman M (2005) AASLD practice guideline: management of hepatocellular carcinoma. Hepatology 42:1208–1236
2. Bruix J, Sherman M (2011) AASLD practice guideline: management of hepatocellular carcinoma: an update. Hepatology 53:1020–1022
3. Bruix J, Sherman M, Llovet JM et al (2001) Clinical management of hepatocellular carcinoma: conclusions of the Barcelona-2000 EASL conference. J Hepatol 35:421–430
4. Torzilli G, Minagawa M, Takayama T et al (1999) Accurate preoperative evaluation of liver mass lesions without fine-needle biopsy. Hepatology 30:889–893
5. Levy I, Greig PD, Gallinger S et al (2001) Resection of hepatocellular carcinoma without preoperative tumour biopsy. Ann Surg 234:206–209
6. Schuhrnann-Giarnpieri C, Schmitt-Willich H, Press WR et al (1992) Preclinical evaluation of Gd-EOB-DTPA as a contrast agent in MR imaging of the hepatobiliary system. Radiology 183:59–64
7. Clement O, Mühler A, Vexler V et al (1992) Gadolinium-ethoxybenzyl-DTPA: a new liver-specific magnetic resonance contrast agent-kinetic and enhancement patterns in normal and cholestatic rats. Invest Radiol 27:612–619
8. Mühler A, Clément O, Saeed M et al (1993) Gadolinium-ethoxybenzyl-DTPA: a new liver-directed magnetic resonance contrast agent-absence of acute epatotoxic, cardiovascular, or immunologic effects. Invest Radiol 28:26–32
9. Weinmann HJ, Schuhmann-Gampieri G, Schmitt-Willich H et al (1991) A new lipophilic gadolinium chelate as a tissue-specific contrast medium for MRI. Magn Reson Med 22:222–228
10. MuehlerA HI, Weinmann HJ (1994) Elimination of Gd-EOB-DTPA in severely impaired liver and kidney excretory function. Invest Radiol 29:213–216
11. Kitao A, Matsui O, Yoneda N et al (2011) The uptake transporter OATP8 expression decreases during multistep hepatocarcinogenesis: correlation with gadoxetic acid enhanced MR imaging. Eur Radiol 21:2056–2066
12. Reimer P, Schneider G, Schima W (2004) Hepatobiliary contrast agents for contrast-enhanced MRI of the liver: properties, clinical development and applications. Eur Radiol 14:559–578
13. Reimer P, Rummeny EJ, Shamsi K et al (1996) Phase II clinical evaluation of Gd-EOB-DTPA: dose, safety aspects and pulse sequence. Radiology 199:177–183
14. Golfieri R, Renzulli M, Lucidi V, Corcioni B, Trevisani F, Bolondi L (2011) Contribution of the hepatobiliary phase of Gd-EOB-DTPA-enhanced MRI to Dynamic MRI in the detection of hypovascular small (≤2 cm) HCC in cirrhosis. Eur Radiol 21:1233–1242
15. Löwenthal D, Zeile M, Lim WY et al (2011) Detection and characterisation of focal liver lesions in colorectal carcinoma patients: comparison of diffusion-weighted and Gd-EOB-DTPA enhanced MR imaging. Eur Radiol 21:832–840
16. Shimada K, Isoda H, Hirokawa Y, Arizono S, Shibata T, Togashi K (2010) Comparison of gadolinium-EOB-DTPA-enhanced and diffusion-weighted liver MRI for detection of small hepatic metastases. Eur Radiol 20:2690–2698
17. Ricke J, Thormann M, Ludewig M et al (2010) MR-guided liver tumour ablation employing open high-field 1.0T MRI for image-guided brachytherapy. Eur Radiol 20:1985–1993
18. Choi JS, Kim MJ, Choi JY, Park MS, Lim JS, Kim KW (2010) Diffusion-weighted MR imaging of liver on 3.0-Tesla system: effect of intravenous administration of gadoxetic acid disodium. Eur Radiol 20:1052–1060
19. Tanimoto A, Lee JM, Murakami T, Huppertz A, Kudo M, Grazioli L (2009) Consensus report of the 2nd International Forum for Liver MRI. Eur Radiol 19:S975–S989
20. Zech CJ, Grazioli L, Jonas E et al (2009) Health-economic evaluation of three imaging strategies in patients with suspected colorectal liver metastases: Gd-EOB-DTPA-enhanced MRI vs. extracellular contrast media-enhanced MRI and 3-phase MDCT in Germany, Italy and Sweden. Eur Radiol 19:S753–S763
21. Reimer P, Rummeny EJ, Daldrup HE et al (1997) Enhancement characteristics of liver metastases, hepatocellular carcinomas, and hemangiomas with Gd-EOB-DTPA: preliminary results with dynamic MR imaging. Eur Radiol 7:275–280
22. Ichikawa T, Saito K, Yoshioka N et al (2010) Detection and characterization of focal liver lesions: a Japanese phase III, multicenter comparison between gadoxetic acid disodium-enhanced magnetic resonance imaging and contrast-enhanced computed tomography predominantly in patients with hepatocellular carcinoma and chronic liver disease. Invest Radiol 45:133–141

23. Kim SH, Kim SH, Lee J et al (2009) Gadoxetic acid-enhanced MRI versus triple-phase MDCT for the preoperative detection of hepatocellular carcinoma. AJR Am J Roentgenol 192:1675–1681
24. Kim YK, Kim CS, Han YM et al (2009) Detection of hepatocellular carcinoma: gadoxetic acid-enhanced 3-dimensional magnetic resonance imaging versus multi-detector row computed tomography. J Comput Assist Tomogr 33:844–850
25. Hammerstingl R, Huppertz A, Breuer J et al (2008) Diagnostic efficacy of gadoxetic acid (Primovist)-enhanced MRI and spiral CT for a therapeutic strategy: comparison with intraoperative and histopathologic findings in focal liver lesions. Eur Radiol 18:457–467
26. Halavaara J, Breuer J, Ayuso C et al (2006) Liver tumour characterization: comparison between liver-specific gadoxetic acid disodium-enhanced MRI and biphasic CT-a multicenter trial. J Comput Assist Tomogr 30:345–354
27. Huppertz A, Balzer T, Blakeborough A et al (2004) Improved detection of focal liver lesions at MR imaging: multicenter comparison of gadoxetic acid-enhanced MR images with intraoperative findings. Radiology 230:266–275
28. Huppertz A, Haraida S, Kraus A et al (2005) Enhancement of focal liver lesions at gadoxetic acid-enhanced MR imaging: correlation with histopathologic findings and spiral CT-initial observations. Radiology 234:468–478
29. Vogl TJ, Kümmel S, Hammerstingl R et al (1996) Liver tumours: comparison of MR imaging with Gd-EOB-DTPA and Gd-DTPA. Radiology 200:59–67
30. Bluemke DA, Sahani D, Amendola M et al (2005) Efficacy and safety of MR imaging with liver-specific contrast agent: U.S. multicenter phase III study. Radiology 237:89–98
31. Akai H, Kiryu S, Takao H et al (2009) Efficacy of double-arterial phase gadolinium ethoxybenzyl diethylenetriamine pentaacetic acid-enhanced liver magnetic resonance imaging compared with double-arterial phase multi-detector row helical computed tomography. J Comput Assist Tomogr 33:887–892
32. Murakami T, Takamura M, Kim T et al (2005) Double phase CT during hepatic arteriography for diagnosis of hepatocellular carcinoma. Eur J Radiol 54:246–252
33. Iannaccone R, Laghi A, Catalano C et al (2005) Hepatocellular carcinoma: role of unenhanced and delayed phase multidetector row helical CT in patients with cirrhosis. Radiology 234:460–467
34. Hayat MA (2009) Methods of cancer diagnosis, therapy, and prognosis. Volume 5, Liver Cancer. Springer, New York, pp 221–235
35. Murakami T, Kim T, Takamura M et al (2001) Hypervascular hepatocellular carcinoma: detection with double arterial phase multi-detector row helical CT. Radiology 218:763–767
36. Tsuboyama T, Onishi H, Kim T et al (2010) Hepatocellular carcinoma: hepatocyte-selective enhancement at gadoxetic acid-enhanced MR imaging–correlation with expression of sinusoidal and canalicular transporters and bile accumulation. Radiology 255:824–833
37. Kogita S, Imai Y, Okada M et al (2010) Gd-EOB-DTPA-enhanced magnetic resonance images of hepatocellular carcinoma: correlation with histological grading and portal blood flow. Eur Radiol 20:2405–2413
38. Fleiss JL (1981) The measurement of interrater agreement. In Statistical methods for rates and proportions. 2nd ed., Wiley, New York, pp 212–236
39. Chakraborty DP, Winter LH (1990) Free-response methodology: alternate analysis and a new observer-performance experiment. Radiology 174:873–881
40. Doo KW, Lee CH, Choi JW et al (2009) "Pseudo washout" sign in high-flow hepatic hemangioma on gadoxetic acid contrast-enhanced MRI mimicking hypervascular tumour. Am J Roentgenol 193: W490–496
41. Sun HY, Lee JM, Shin CI et al (2010) Gadoxetic acid-enhanced magnetic resonance imaging for differentiating small hepatocellular carcinomas (2 cm in diameter) from arterial enhancing pseudolesions: special emphasis on hepatobiliary phase imaging. Invest Radiol 45:96–103
42. Marin D, Di Martino M, Guerrisi A et al (2009) Hepatocellular carcinoma in patients with cirrhosis: qualitative comparison of gadobenate dimeglumine-enhanced MR imaging and multiphasic 64-section CT. Radiology 251:85–95